5.4

A SUMMARY OF DATA COLLECTED DURING VORTEX2 BY MWR-05XP/TWOLF, UMASS X-POL, AND THE UMASS W-BAND RADAR

Howard B. Bluestein*, M. M. French, J. B. Houser, J. C. Snyder, R. L. Tanamachi
School of Meteorology, University of Oklahoma, Norman

I. PopStefanija and C. Baldi
ProSensing, Inc., Amherst, Massachusetts

G. D. Emmitt
Simpson Weather Associates, Charlottesville, Virginia

V. Venkatesh, K. Orzel, and S. J. Frasier
Microwave Remote Sensing Laboratory, University of Massachusetts, Amherst

R. T. Bluth
CIRPAS, Naval Postgraduate School, Monterey, California

1. INTRODUCTION

During VORTEX2, three scanning, mobile, truck-mounted Doppler radars and a mobile, scanning Doppler lidar were used in the field by a group of faculty and graduate students from the University of Oklahoma (OU), supported by personnel from the institutions given above. These platforms were part of the VORTEX2 armada. A scout car from OU assisted with field operations.

The U. Mass. W-band radar (Fig. 1) (e.g., Bluestein et al. 2007a) has been used since 1993. It has a half-power beamwidth of 0.18^0 and is used mainly to probe tornadoes at high spatial resolution, near the ground, from a range of 10 - 15 km or less.

The U. Mass. X-Pol radar (Fig. 2) is an X-band, polarimetric radar, whose antenna has a half-power beamwidth of 1.25^0. It has been used since 2001 without Doppler or polarimetric capability and since 2002 with both Doppler and polarimetric capabilities (e.g., Bluestein et al. 2007b). During VORTEX2 it was used to complement the other X-band radars for multiple Doppler analysis, for continuous surveillance, and to identify polarimetric signatures in supercells (Snyder et al. 2010).

Figure 1. U. Mass. W-band radar probing a tornado in Goshen County, Wyoming on 5 June 2009. © R. Tanamachi

The MWR-05XP (Fig. 3) is an X-band, phased-array radar, having a half-power beamwidth of 1.8^0 and 2^0 in the horizontal and vertical, respectively (Bluestein et al. 2010). It has been used since 2007 to map out the wind field in volumetric sectors of severe convective storms with updates in 2010 as short as 6 – 7 s.

* *Corresponding author address:* Howard B. Bluestein, School of Meteorology, University of Oklahoma, Norman, OK 73072; e-mail: hblue@ou.edu

Figure 2. U. Mass. X-Pol probing a tornado in Goshen County, Wyoming on 5 June 2009. © J. Snyder

Figure 3. MWR-05XP probing a tornado in Goshen County, Wyoming on 5 June 2009. © C. Baldi

TWOLF (Truck-Mounted Wind-Observing Facility) is a Coherent Technologies 2 μm, eye-safe, pulsed Doppler lidar (Fig. 4) mounted on the MWR-05XP truck. It was used for the first time during year 2 (2010) of VORTEX2. It was used to add coverage in clear air between the radar and the precipitation in supercells and to detect boundary-layer features just upstream from the main updraft in supercells. Its range varies with the amount of aerosol, but is generally 10 – 15 km in the clear-air boundary layer.

Figure 4. TWOLF mounted on the MWR-05XP radar truck, next to the phased-array antenna (orange). © H. Bluestein

The main purpose of this paper is to show examples of some of the data collected and summarize the highlights of phenomena documented, with the hope that in addition to the authors, who will be analyzing some of the radar and lidar data collected, other investigators will also make use of some of the data for their studies.

2. EXAMPLES OF DATA COLLECTED

The most significant datasets collected are highlighted in Figs. 5 – 31. Cases range from the documentation of the entire life cycle of tornadoes on 5 June 2009, 10 May

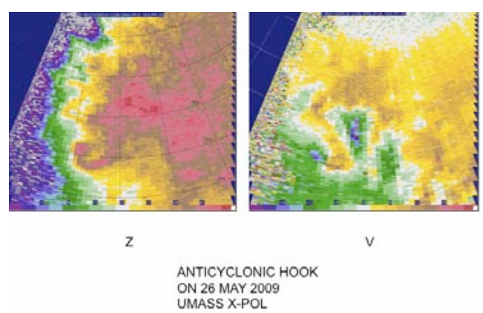

Figure 5. Mid-level anticyclonic hook (left) and anticyclonic-shear signature (right) as detected by U. Mass. X-Pol, on 26 May 2009 in north-central Texas.

Figure 6. Ultra-wide view of the tornado, wall cloud, and flanking line in the Goshen County supercell on 5 June 2009. © H. Bluestein

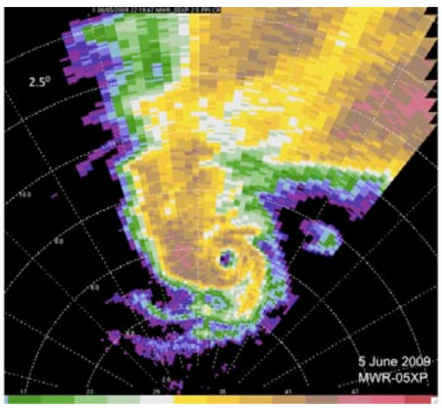

Figure 7. Close-range, low-level reflectivity associated with the Goshen County tornado, as seen by the MWR-05XP. Note the weak-echo eye and spiral bands in the clear-air boundary layer surrounding the tornado.

2010, and 25 May 2010 through volumetric radar scans at 6 – 10 s update times, to single-elevation scans of gustnadoes and landspouts. A wealth of polarimetric data was collected in supercells and in and near tornadoes. Small-scale vortices (too weak to be considered tornadoes) in supercells were documented by the W-band radar; ultra-fine-scale boundary-layer streaks/rolls were documented by the Doppler lidar (TWOLF).

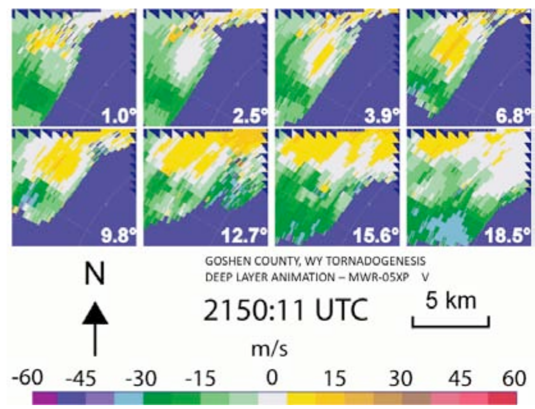

Figure 8. Doppler velocity at selected elevation angles just prior to tornadogenesis in the Goshen County, Wyoming supercell, as seen by the MWR-05XP.

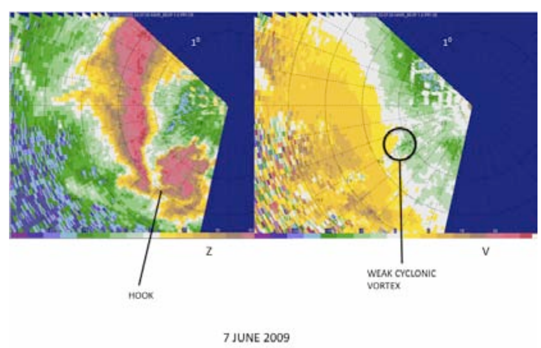

Figure 9. Hook echo (left) and Doppler velocity (right) at low levels in a large-hail producing supercell in NW Missouri on 7 June 2009, as seen by the MWR-05XP.

Figure 10. Sequence of photos showing the dissipation of a supercell in SW Kansas on 9 June 2009. The MWR-05XP is seen in the upper-left panel. © H. Bluestein

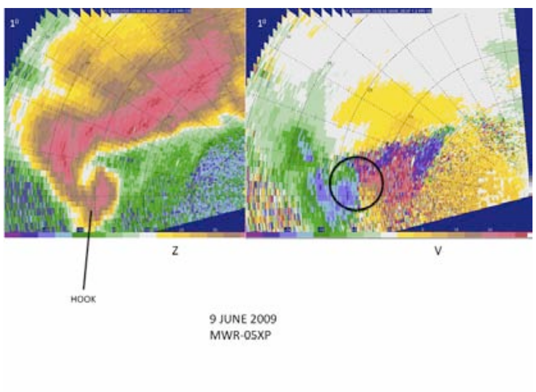

Figure 11. Hook echo (left) and Doppler velocity (right) in the supercell seen in Fig. 10, upper left, from the MWR-05XP.

Figure 12. HP supercell in SE Colorado on 11 June 2009. MWR-05XP is seen probing the supercell in the lower-right panel. © H. Bluestein

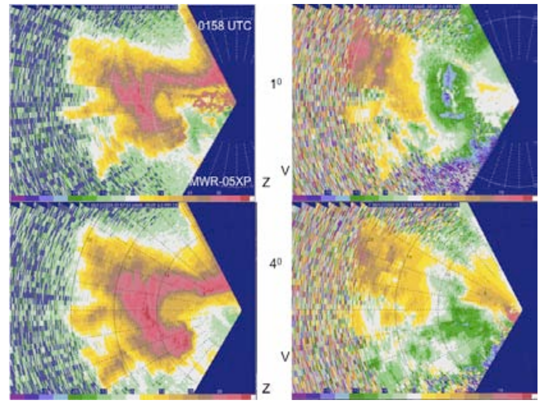

Figure 13. Hook echo (left panels) and Doppler velocity (right panels) at low (top row) and higher (bottom row) of the HP supercell seen in Fig. 12, from data collected by the MWR-05XP.

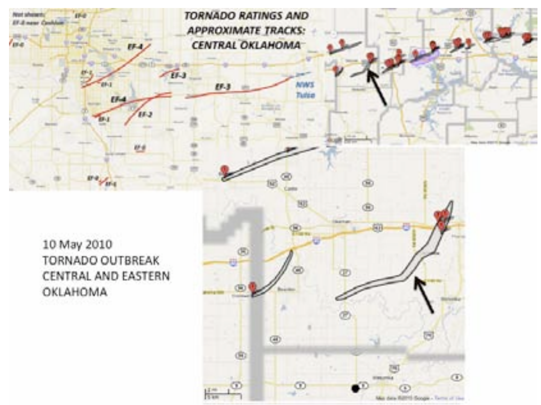

Figure 14. Damage maps of some of the tornadoes in central Oklahoma on 10 May 2010, courtesy of the NWS offices in Norman and Tulsa. The arrow marks the damage path of the tornado probed by the MWR-05XP and U. Mass. X-Pol. Location of former is given by the thick dot.

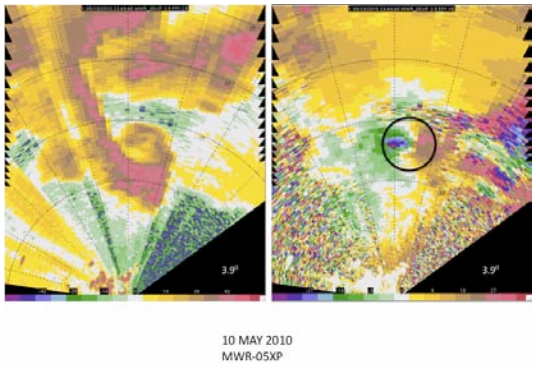

Figure 15. Hook echo (left) and cyclonic-vortex signature (right) associated with the "Clearview, OK" tornado (cf. Fig. 14), as seen by the MWR-05XP at 3.9^0 elevation angle.

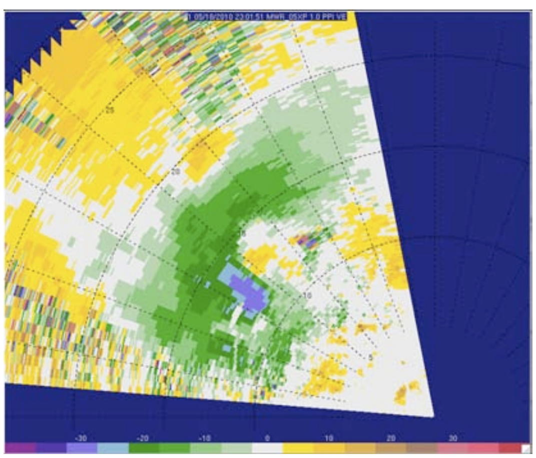

Figure 16. Doppler-velocity field showing a strong, low-level cyclonic-vortex signature (purple – yellow) in an HP supercell in the N Texas Panhandle on 18 May 2010, as detected by the MWR-05XP.

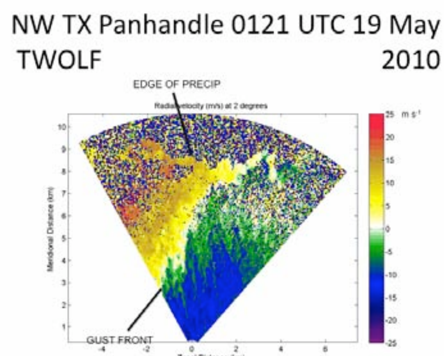

Figure 17. Doppler-velocity field in the inflow region at low levels ahead of the HP supercell in the N Texas Panhandle on 18 May 2010 (much later than that depicted in Fig. 16), as seen by TWOLF.

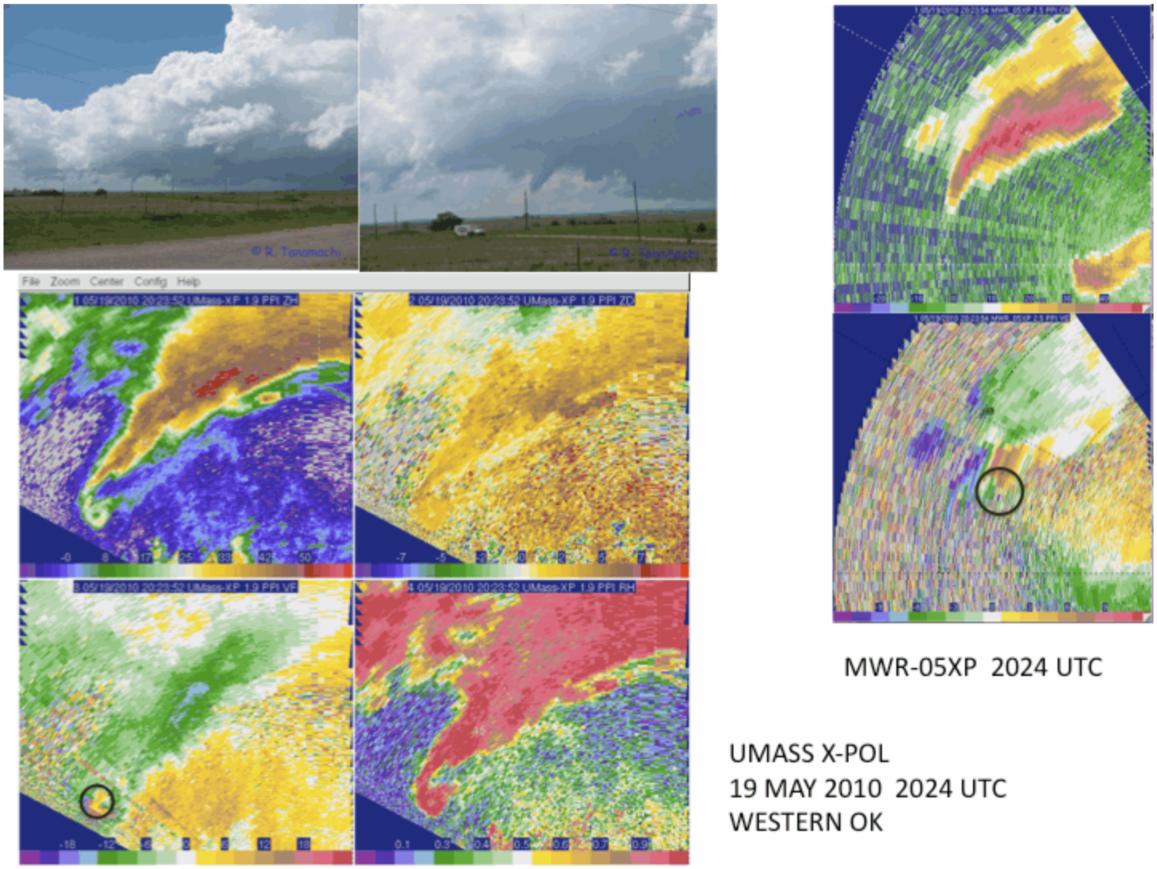

Figure 18. Photographs of the first tornado in a supercell in W Oklahoma on 19 May 2010 (upper left; © R. Tanamachi). Coincident reflectivity, Z_{dr}, ρ_{hv}, and Doppler velocity fields, displayed in a clockwise manner, from the U. Mass. X-Pol (lower left four panels), and reflectivity and Doppler velocity (upper right two panels) from the MWR-05XP.

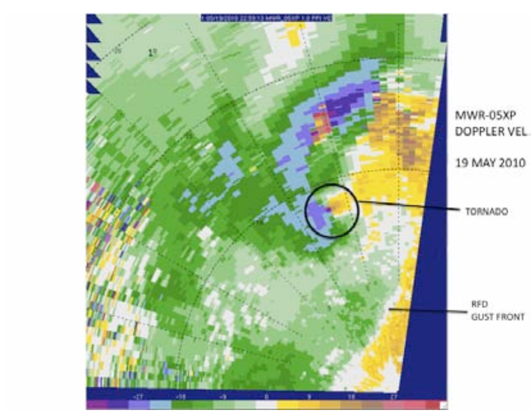

Figure 19. Doppler velocity field at low elevation angle in the vicinity of the tornado in an HP supercell near Kingfisher, Oklahoma on 19 May 2010, as seen by the MWR-05XP.

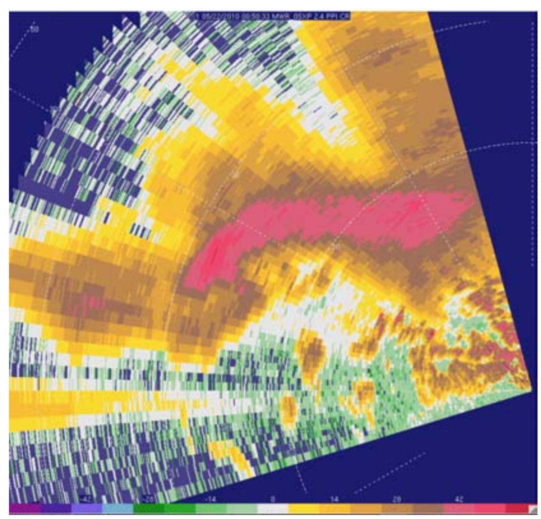

Figure 20. Reflectivity field at low-levels of a non-tornadic supercell in far NW Nebraska on 21 May 2010, as seen by the MWR-05XP.

Figure 21. One of a series of tornadoes in a supercell in far western Kansas near the Colorado border (NW of Tribune, Kansas) on 25 May 2010. © H. Bluestein

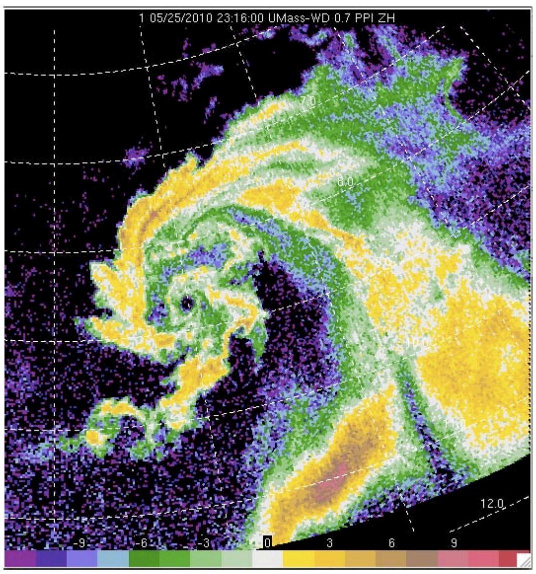

Figure 22. The beginning of the tornado seen in Fig. 21, as depicted by low-level reflectivity from the U. Mass. W-band radar.

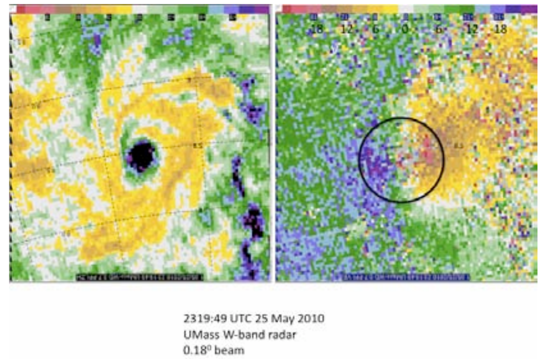

Figure 23. Expanded view of low-level reflectivity (left) and Doppler velocity (right) in the tornado seen in Fig. 21, as detected by the U. Mass. W-band radar.

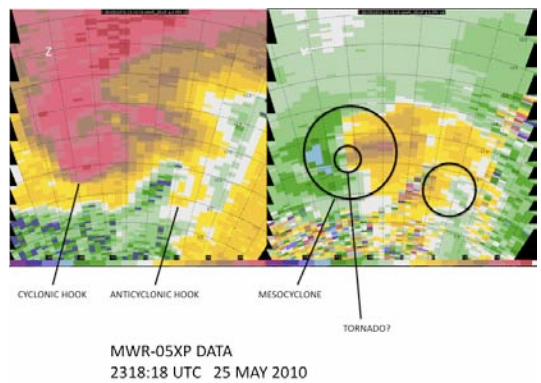

Figure 24. Radar reflectivity (left) and Doppler velocity (right) at low levels of the tornado seen in Fig. 21, and of an anticyclonic hook and anticyclonic shear signature, as viewed by the MWR-05XP.

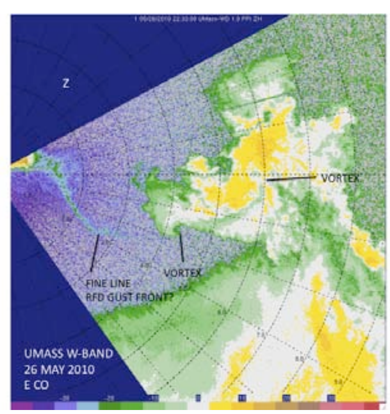

Figure 25. Radar reflectivity of features at low levels in a supercell in E Colorado on 26 May 2010, as seen by the U. Mass. W-band radar.

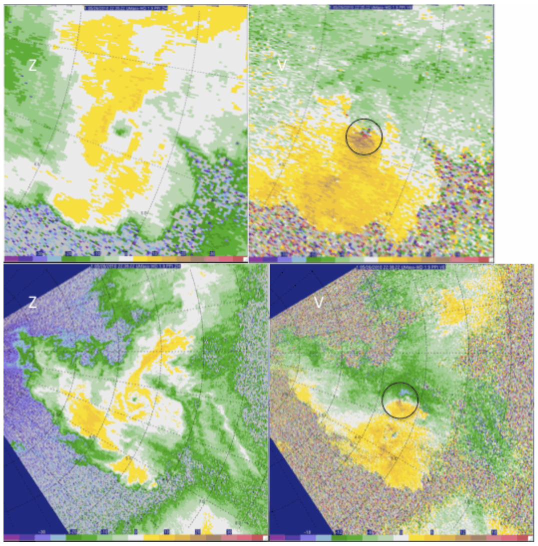

Figure 26. Expanded views of reflectivity (left) and Doppler velocity (right) of low-level vortices detected by the U. Mass. W-band radar in E Colorado on 26 May 2010.

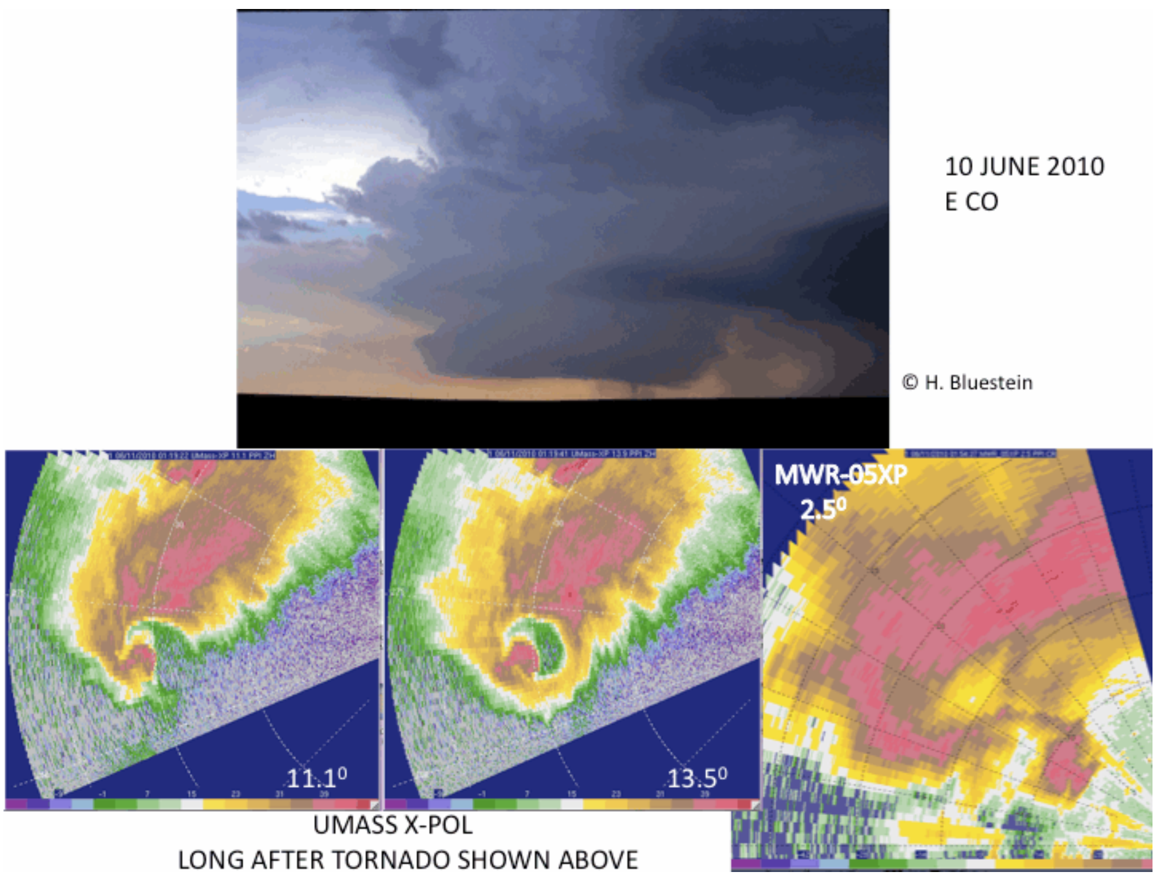

Figure 27. Supercell with a tornado near Last Chance, Colorado, on 10 June 2010 (top, © H. Bluestein); hook echo (lower left) and crescent-shaped BWER (lower, middle) of the supercell later on, from U. Mass. X-Pol; low-level reflectivity of hook echo in the same supercell a short time later, from the MWR-05XP.

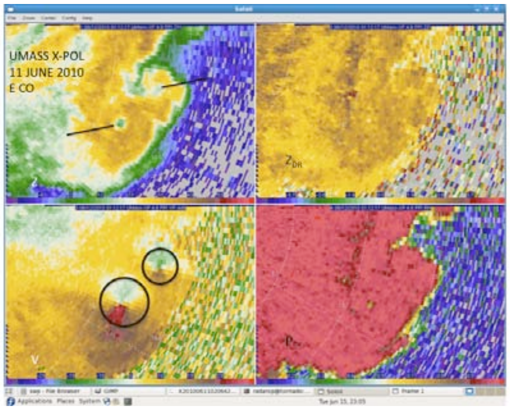

Figure 28. Two tornadoes detected by the U. Mass. X-Pol in E Colorado on 11 June 2010. Reflectivity (upper left); Z_{dr} (upper right); Doppler velocity (lower left); ρ_{hv} (lower right).

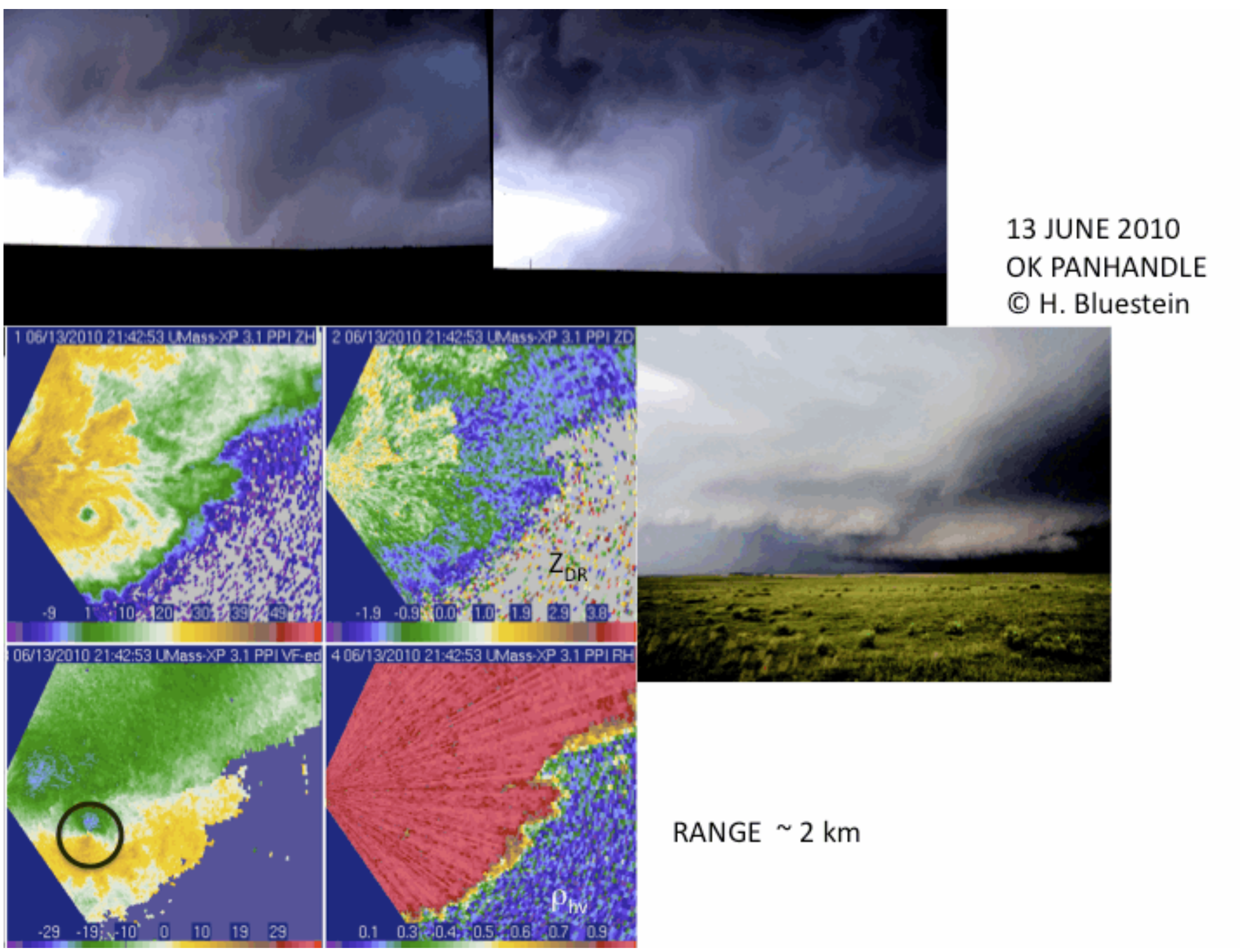

Figure 29. Tornado in the eastern Oklahoma Panhandle on 13 June 2010 (top two panels; © H. Bluestein). Lower-left four panels: Reflectivity (upper left); Z_{dr} (upper right); Doppler velocity (lower left); ρ_{hv} (lower right) as seen by the U. Mass. X-Pol. Wall cloud and tail cloud in the tornadic, HP supercell (right-center; © H. Bluestein).

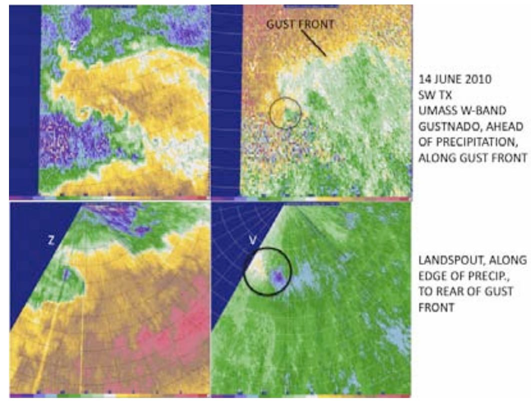

Figure 31. Gustnado along the leading edge of the outflow for the storm shown in Fig. 30 (upper left, reflectivity; upper right (Doppler velocity). Landspout well behind the leading gust front (lower left, reflectivity; lower right, Doppler velocity). As seen by the U. Mass. W-band radar at low levels.

Figure 30. Severe convective storm near Tahoka, Texas, on 14 June 2010 (top; © H. Bluestein). Landspouts along the cloud base, well behind the leading gust front (bottom; © H. Bluestein)

3. SUMMARY

Highlights from both years of VORTEX2 are given in Tables 1 and 2. The most significant cases are identified in the tables by arrows. More detailed information is contained in the VORTEX2 field catalog online at http://catalog.eol.ucar.edu/cgi-bin/vortex2_2010/report/index. Potential collaborators are encouraged to contact the authors. Analyses of some of the cases have begun.

Table. Highlights of Year 1 of VORTEX-2

Date (2009)	X-Pol	W-band	MWR-05XP	Description
8 May	X	X	X	Test; supercell in S Cen OK
12 May	X	NA	X	gust front, multicell in TX Panhandle
13 May	X	NA	X	HP supercell in Cen OK
15 May	X	X	X	squall line in N Cen OK
19 May	X	X	X	multicell, microbursts in NE
20 May	X	X	X	supercell in NE
22 May	X	X	NA	multicells in NE and SD
23 May	X	X	X	multicell line in NE
25 May	X	NA	X	strong multicell in W OK
26 May	X	NA	X	multicell, supercell with anticyclone, gust front, in N Cen TX
29 May	X	X-	X	multicell in NE
31 May	X	X-	X	multicell in IA
1 June	NA	X-	X	multicells in NE
4 June	X	X-	X	supercell/multicell line in WY
5 June	X	X-	X	complete life cycle of tornado in supercell, in WY; supercell in W NE
6 June	X	X-	X	supercells in NE
7 June	X	X-	X	supercell, very large hail, in NW MO
9 June	X	X-	X	supercell in SW KS
10 June	X	X-	X	multicells in SW KS/SE CO
11 June	NA	NA	X	HP supercell in SE CO
13 June	X	X-	X	supercell in TX Panhandle
14 June	NA	NA	NA	supercell in TX Panhandle

Table 1: Highlights of VORTEX2, year 1

In this table, “X” denotes that useful data were collected, “X-“ denotes that data were collected but the sensitivity of the instrument was below par; these data are only marginally useful. “N/A” indicates that data are not available: The instrument was not collecting data because it was not available, not operational, or, in one case, that data were collected but not recorded properly. In the subsequent table, when the sensitivity of the instrument was very low or if no interesting data were collected owing to beam blockage or inadequate positioning, a blank is used rather than X-.

Highlights of Year 2 of VORTEX2

	Date (2010)	X-Pol	W-band	MWR-05XP	TWOLF	Description
→	10 May	X	N/A	X	X	Tornadic supercell in E OK
	11 May		N/A	X	X	Supercell in NW OK
	12 May	X	N/A	X	X	Supercells in SW and W OK
	14 May	X	N/A	N/A	N/A	Storms in SW TX
	15 May	X	N/A	N/A	N/A	Supercell in SE NM
	17 May	X	N/A	N/A	N/A	Supercell in SE NM
→	18 May	X	N/A	X	X	Supercell in N TX Panhandle
→	19 May	X	N/A	X	X	Tornadic supercells in W OK
	21 May		X*	X	X	Supercell NW NE and *Supercell in TX Panhandle
	23 May	X	X	X	X	Dissipating supercell in W KS
	24 May	X	X	X	X	Line of convection and supercells in SW NE
→	25 May	X	X	X	X	Tornadic supercell in W KS
→	26 May	X	X	X	X	Supercell in E CO
	28 May					Surface boundary in NW NE
	29 May			X	X	Surface boundary and storm in NW NE
	2 June	X	X	X	X	Supercell in NW KS
	3 June	X		X	X	Supercells in NE NE
	5 June					Storms in Central Iowa
	6 June	X	X	X	X	Supercells in SW NE
	7 June	X	X	N/A	X	Supercell/tornadic supercell in E WY/W NE
	9 June	X	X	X	X	Supercell in E WY
→	10 June	X	X	X	X	Supercell and post-tornadic supercell in E CO
→	11 June	X	X	X	X	Tornadic supercell in E CO
	12 June	X	X	N/A	N/A	Embedded supercells in N TX Panhandle
→	13 June	X	X	N/A	N/A	Supercells and tornadic supercell in N TX Panhandle and OK Panhandle
→	14 June	X	X	N/A	N/A	Gustnadoes and landspouts in W TX

Table 2: Highlights of VORTEX2, year 2

4. REFERENCES

Bluestein, H. B., M. M. French, I. PopStefanija, R. T. Bluth, and J. B. Knorr, 2010: A mobile, phased-array Doppler radar for the study of severe convective storms. *Bull. Amer. Meteor. Soc.*, **91**, 579 – 600.

Bluestein, H. B., C. C. Weiss, M. M. French, E. M. Holthaus, R. L. Tanamachi, S. Frasier, and A. L. Pazmany, 2007a: The structure of tornadoes near Attica, Kansas, on 12 May 2004: High-resolution, mobile, Doppler radar observations. *Mon. Wea. Rev.*, **135**, 475 – 506.

Bluestein, H. B., M. M. French, R. L. Tanamachi, S. Frasier, K. Hardwick, F. Junyent, and A. L. Pazmany, 2007b: Close-range observations of tornadoes in supercells made with a dual-polarization, X-band, mobile Doppler radar. *Mon. Wea. Rev.*, **135**, 1522 – 1543.

Snyder, J. C., H. B. Bluestein, G. Zhang, and S. J. Frasier, 2010: Attenuation correction and hydrometeor classification of high-resolution, X-band, dual-polarized mobile radar measurements in severe convective storms. *J. Atmos. Oceanic Technol.* (in press)

5. ACKNOWLEDGMENTS

Data collection and processing were supported by NSF grants ATM-0637148 and AGS-0934307 to the University of Oklahoma, ATM-0641201 and AGS-0937768 to the University of Massachusetts, and by contracts from the Navy SBIR program at ONR to ProSensing, Inc. and Simpson Weather Associates. Bethany Seeger (ProSensing) and Paul Buczynski (NPS), Derek Hutton (Lockheed Martin) and Dan Carre (SWA), Tom Hartley (U. Mass.), and Ogechi Ibe (U. Mass.) provided additional support with the MWR-05XP, TWOLF, U. Mass. W-band radar and U. Mass. X-Pol, respectively. W. – C. Lee and technicians at NCAR/EOL provided some assistance while the MWR-05XP truck had mechanical problems in Colorado. Nick Engerer (OU) drove the OU Scout car.